ACS Medicinal Chemistry Letters

Letter

pubs.acs.org/acsmedchemlett

Discovery and Pharmacological Characterization of Novel Quinazoline-Based PI3K Delta-Selective Inhibitors

Klemens Hoegenauer,*[,†] Nicolas Soldermann,*[,†] Frédéric Stauffer,[†] Pascal Furet,[†] Nadege Graveleau,[†] Alexander B. Smith,[†] Christina Hebach,[†] Gregory J. Hollingworth,[†] Ian Lewis,[†] Sascha Gutmann,[‡] Gabriele Rummel,[‡] Mark Knapp,[⊥] Romain M. Wolf,[†] Joachim Blanz,[§] Roland Feifel,[§] Christoph Burkhart,[∥] and Frédéric Zécri[†]

[†]Global Discovery Chemistry, [‡]Center for Proteomic Chemistry, [§]Metabolism and Pharmacokinetics, [∥]Autoimmunity, Transplantation and Inflammation, Novartis Institutes for BioMedical Research, Novartis Campus, CH-4002 Basel, Switzerland

[⊥]Global Discovery Chemistry, Novartis Institutes for BioMedical Research, 5300 Chiron Way, Emeryville, California 94608, United States

Supporting Information

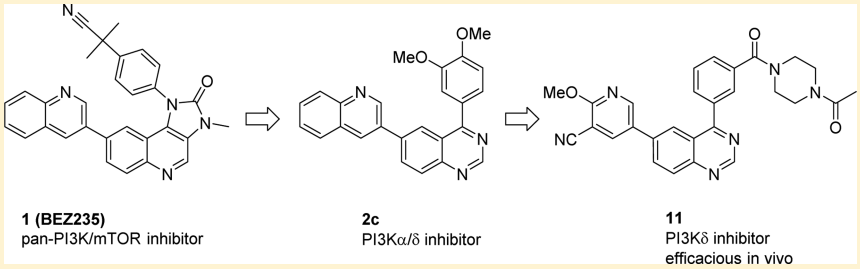

ABSTRACT: Inhibition of the lipid kinase PI3Kδ is a promising principle to treat B and T cell driven inflammatory diseases. Using a scaffold deconstruction−reconstruction strategy, we identified 4-aryl quinazolines that were optimized into potent PI3Kδ isoform selective analogues with good pharmacokinetic properties. With compound **11**, we illustrate that biochemical PI3Kδ inhibition translates into modulation of isoform-dependent immune cell function (human, rat, and mouse). After oral administration of compound **11** to rats, proximal PD markers are inhibited, and dose-dependent efficacy in a mechanistic plaque forming cell assay could be demonstrated.

KEYWORDS: *Phosphoinositide-3-kinase delta inhibitor, PI3Kδ inhibitor, lead optimization, structure−activity relationship, PK/PD studies, B cell inhibition*

Phosphoinositide-3-kinases (PI3Ks) are lipid kinases responsible for the generation of the second messenger phosphatidylinositol (3,4,5) triphosphate (PIP3) from the substrate phosphatidylinositol (4,5) biphosphate (PIP2) leading to phosphorylation of Akt and subsequent progression of cell differentiation, proliferation, motility, and survival.[1,2] PI3Ks have been classified according to their structural and functional properties. The class I enzymes can be divided into IA and IB PI3K. In mammals, class IA PI3K includes three different isoforms: PI3Kα, PI3Kβ, and PI3Kδ, while class IB includes PI3Kγ. These enzymes are heterodimers consisting of the p110 catalytic subunits (p110α, p110β, p110γ, and p110δ) and a regulatory subunit (most commonly p85α).[3]

During the past decade there has been a great deal of interest in the development of inhibitors of the class I PI3K family. Initially, broad-spectrum inhibitors of the α, β, γ, and δ isoforms were targeted as potential oncology therapeutics.[4−6] However, the recognition that the γ and δ isoforms are predominantly expressed in leukocytes and play a critical role in T and B cell function[7] led to speculation that selective inhibitors of these isoforms could offer potential as therapeutics for the treatment of allergic and inflammatory diseases.[8] Moreover, specifically targeting PI3Kδ should avoid potential side effects associated with the ubiquitously expressed PI3Kα and β isoforms.[9−11] PI3Kδ is expressed primarily in hematopoietic cells, and its functional relevance in the activation of leukocytes of the adaptive as well as the innate immune system has been demonstrated in genetically modified mice (PI3K$\delta^{D910A/D910A}$ knock-in and PI3K$\delta^{-/-}$)[12−14] and through the use of specific tool compounds in in vitro and in vivo preclinical models.[15−17] The strong biological rationale led us and others[18−21] to initiate a medicinal chemistry program aimed at the discovery of PI3Kδ-selective inhibitors with suitable properties and efficacy to allow for development as an anti-inflammatory therapeutic.

Our efforts toward the identification of PI3K inhibitors, which are selective for the delta isoform, started with imidazoquinoline **1** (BEZ235, Table 1), a pan-PI3K/mTOR inhibitor with potent

Received: March 17, 2016
Accepted: June 2, 2016
Published: June 2, 2016

DOI: 10.1021/acsmedchemlett.6b00119
ACS Med. Chem. Lett. 2016, 7, 762−767

Table 1. Influence of Position-4 Substituents of the Quinazoline on Overall Potency, PI3K Isoform Selectivity, and Selectivity Towards mTOR

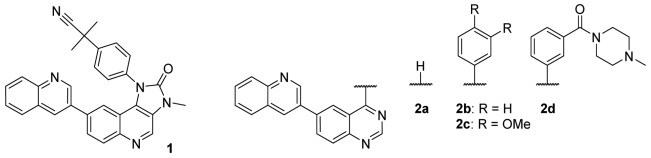

	biochemical IC_{50} [μM][a]				
	PI3Kα[b]	PI3Kβ[b]	PI3Kγ[c]	PI3Kδ[c]	mTOR[d]
1	0.017	0.192	0.313	0.025	0.006
2a	0.650	>10	>10	8.1	>10
2b	0.090	3.2	5.6	0.320	0.66
2c	0.095	1.9	2.6	0.061	1.8
2d	0.633	>10	>10	0.049	5.3

[a]Mean of a minimum of two independent experiments; standard deviation for pIC_{50} values <0.3. [b]KGlo format. [c]ADAPTA format (values comparable to KGlo). [d]Radiometric protein kinase assay.

antitumor activity.[22] We had a good understanding of the binding mode of imidazoquinoline **1** based on docking studies of numerous compounds of this scaffold into a homology model of PI3Kα, which was built based on the reported X-ray structure of PI3Kγ kinase domain.[23] Using a similar homology model for PI3Kδ, we hypothesized that we would gain selectivity by reaching out to the nonconserved amino acid residues that line the entrance of the ATP binding site (see Supplementary Figure 3). To this end, we first deconstructed the imidazoquinoline to the quinazoline fragment **2a** (Table 1) to remove the structural elements, which interact in the selectivity pocket and contribute significantly to the strong affinity for mTOR. Quinazoline **2a** contains some crucial core elements for PI3K binding affinity, namely, the position-1 nitrogen acting as a hinge binder and the quinoline, which fills the affinity-pocket (conserved over all PI3K isoforms). We detected submicromolar activity for PI3Kα, only, making this compound a very ligand efficient PI3Kα inhibitor. Some marginal activity on PI3Kδ was retained, while the affinity toward all other PI3K isoforms as well as mTOR was above the highest test concentration. Introduction of a 4-phenyl substituent (**2b**) increased the activity for PI3Kα and δ considerably with some emerging selectivity over the β and γ isoforms. Modification of the substitution pattern of the phenyl group led to some additional favorable modulation of the PI3Kδ (higher) and mTOR (lower) activity, exemplified by dimethoxyphenyl analogue **2c**. Modeling suggested that the best exit vector to selectively interfere with the nonconserved residues at the entrance of the PI3K ATP binding site (selectivity pocket) would be from the meta-position of the newly introduced phenyl group. In particular, our intention was to form a salt bridge with the nonconserved D832 side chain of the PI3Kδ isoform with a hydrogen bond donor (e.g., a protonated amine) on the ligand (see Supplementary Figure 3). We probed this concept with a small library and in that way identified piperazine amide **2d** as a lead compound, demonstrating potency on PI3Kδ and significant selectivity over all other Class I PI3K isoforms as well as mTOR. Based on these encouraging results, we began to optimize substituents of the quinazoline in positions 4 and 6 (for synthetic details, see Supporting Information).

Table 2 shows that the biochemical activity of piperazine amide **2d** translates well to Rat-1 cells that have been transfected with myristoylated, and therefore constitutively active, PI3Kα, β, and δ isoforms without significant activity drop. Isoform selectivity observed for biochemical assays is maintained in the cellular assays. The cellular activity on PI3Kδ was also replicated in murine splenocytes (measured as inhibition of anti-IgM-induced expression of the costimulatory molecule CD86 on B cells), yet a

Table 2. Influence of Position-4 and -6 Substituents of the Quinazoline on Biochemical/Cellular Potency, PI3K Isoform Selectivity, hERG Inhibition, and in Vitro ADME Parameters

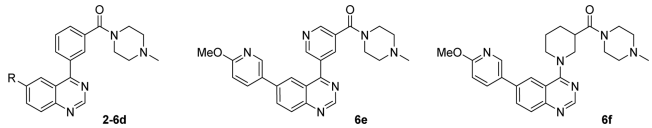

	R	biochemical IC_{50} [μM][a]				cellular IC_{50} [μM][a,d]			mCD86 IC_{50} [μM][a,e]	PAMPA $logP_e$[f]	hERG IC_{50} [μM][g]	HT-logP[h]	RLM CL_{int}[i]	HT-sol[j]
		PI3Kα[b]	PI3Kβ[b]	PI3Kγ[c]	PI3Kδ[c]	PI3Kα	PI3Kβ	PI3Kδ						
2d	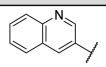	0.633	>10	>10	0.049	1.14	>12.5	0.038	0.190	-3.9	2.6	3.1	>700	>1.0
3d	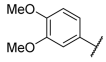	0.410	2.57	0.740	0.014	1.09	4.89	0.018	0.026	-4.1	1.9	2.8	357	0.85
4d	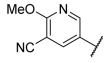	0.283	2.63	9.2	0.027	1.56	1.91	0.037	0.087	-4.2	11	1.9	231	0.42
5d	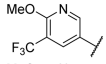	0.079	0.392	9.3	0.009	0.40	0.38	0.010	0.074	-3.6	1.6	3.9	213	0.85
6d	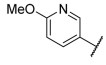	0.259	4.15	7.9	0.020	1.56	1.91	0.037	0.087	-3.7	12	2.2	605	>1.0
6e		0.462	6.18	>10	0.100[k]	2.49	7.54	0.036	0.112	-4.4	26	1.9	201	>1.0
6f		0.399	2.04	4.5	0.064[k]	1.82	4.62	0.070	0.086	-3.8	1.5	nd[l]	130	>1.0

[a]Mean of a minimum of two independent experiments; standard deviation for pIC_{50} values <0.3. [b]KGlo format. [c]ADAPTA format (values comparable to KGlo). [d]Inhibition of pAkt formation in Rat-1 cells. [e]Inhibition of anti-IgM induced mCD86 expression on mouse splenocytes. [f]Effective permeability [10^{-6} cm·s^{-1}] (pH = 6.8), n = 1. [g]Inhibition of [^3H]dofetilide binding to hERG transfected membranes, n = 1. [h]High-throughput logP measurement with immobilized artificial membranes, n = 1. [i]Intrinsic clearance in incubations of rat liver microsomes [μL·min^{-1}·mg^{-1} protein], n = 1. [j]High-throughput equilibrium solubility determination [mM] (pH = 6.8). [k]Low Hill coefficient. [l]nd = not determined.

DOI: 10.1021/acsmedchemlett.6b00119
ACS Med. Chem. Lett. 2016, 7, 762−767

Table 3. Influence of Position-6 Substituents of the Quinazoline on Biochemical/Cellular Potency, PI3K Isoform Selectivity, hERG Inhibition, and in Vitro ADME Parameters

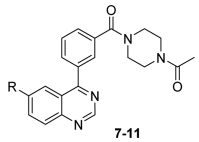

7-11

	R	biochemical IC_{50} [μM][a]				cellular IC_{50} [μM][a,d]			mCD86 IC_{50} [μM][a,e]	PAMPA $logP_e$[f]	hERG IC_{50} [μM][g]	HT-logP[h]	RLM CL_{int}[i]	HT-sol[j]
		PI3Kα[b]	PI3Kβ[b]	PI3Kγ[c]	PI3Kδ[c]	PI3Kα	PI3Kβ	PI3Kδ						
7		0.829	4.27	5.6	0.003	2.10	4.65	0.062	0.393	-5.3	>30	2.8	525	0.61
8	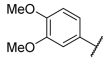	0.127	1.94	0.220	0.014	1.32	3.38	0.039	0.034	-5.1	>30	1.9	68	0.80
9	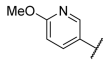	0.418	4.84	2.7	0.029	2.12	3.57	0.028	0.070	-4.9	>30	2.7	115	>1.0
10	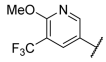	0.084	0.536	1.4	0.005	0.690	2.07	0.014	0.093	-4.1	>30	3.1	83	0.38
11	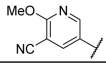	0.262	1.65	4.63	0.009	3.44	6.53	0.049	0.074	-5.5	>30	2.8	63	0.21

[a]Mean of a minimum of two independent experiments; standard deviation for pIC_{50} values <0.3. [b]KGlo format. [c]ADAPTA format (values comparable to KGlo). [d]Inhibition of pAkt formation in Rat-1 cells. [e]Inhibition of anti-IgM induced mCD86 expression on mouse splenocytes. [f]Effective permeability [10^{-6} cm·s^{-1}] (pH = 6.8), n = 1. [g]Inhibition of [^3H]dofetilide binding to hERG transfected membranes, n = 1. [h]High-throughput logP measurement with immobilized artificial membranes, n = 1. [i]Intrinsic clearance in incubations of rat liver microsomes [μL·min^{-1}·mg^{-1} protein], n = 1. [j]High-throughput equilibrium solubility determination [mM] (pH = 6.8).

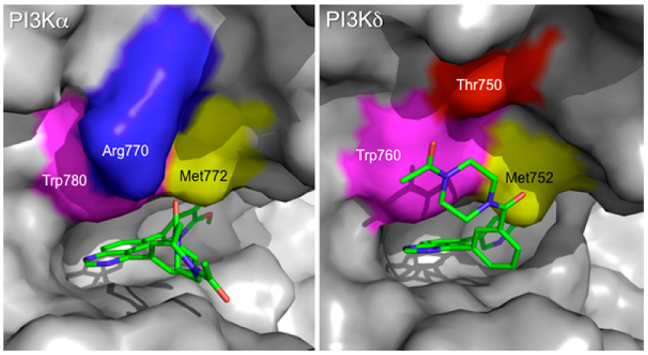

Figure 1. Cocrystal structures of PI3K*α* (left panel) and PI3K*δ* (right panel) in complex with compound **11**. The protein is shown as gray surface and the inhibitor is represented as green sticks. Whereas compound **11** stacks onto W760 in PI3K*δ*, R770 in PI3K*α* forces the inhibitor to adopt an extended conformation. Key amino acid residues are highlighted in color.

Table 4. Cellular Inhibition of PI3K*δ*-Dependent B Cell Activation in Different Species by Compound 11

biochemical IC_{50} [μM][a]						
human[b]			rat[c]		mouse[d]	
pAkt	CD86	CD69	pAkt	CD86	prolif.	CD86
0.029	0.107	0.125	0.089	0.044	0.011	0.070

[a]Mean of a minimum of two independent experiments; standard deviation for pIC_{50} values <0.3. [b]Measured in 90% whole blood. [c]Measured in 50% whole blood. [d]Measured in splenocytes.

ca. 5-fold activity drop was observed. Due to its moderate lipophilicity and positive charge, piperazine amide **2d** is very soluble at neutral pH. Areas identified for improvement were interference with the hERG channel and metabolic instability in rat liver microsomes.

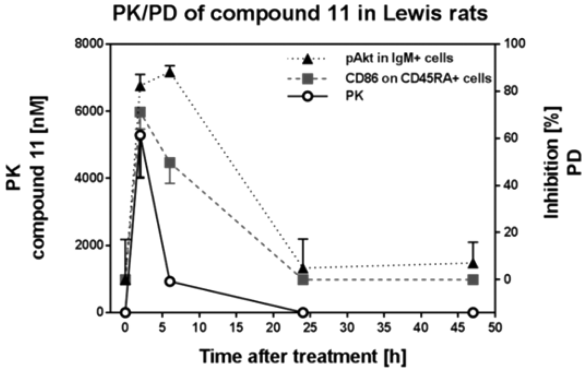

Figure 2. Rat PK/PD for compound 11 at 30 mg/kg p.o. single dose: inhibition of ex vivo induced B cell activation in 50% whole blood; PK legend at the left, PD legend at the right; error bars indicate standard deviation.

We found that the activity on PI3K*δ* could be preserved to a large extent by replacing the position-6 quinoline motif of **2d** with less lipophilic monocyclic features. A selection of these analogues is shown in Table 2 (compounds **3d**−**6d**). Whereas compounds **3d**, **4d**, and **6d** still displayed significant selectivity toward the other PI3K isoforms, introduction of a *meta*-CF_3 substituent (**5d**) led to a potency increase of PI3K*α* and *β* in addition to a substantial rise in log P. Further translation of the cellular response to the splenocyte assay was generally better for less lipophilic derivatives, perhaps due to less unspecific binding to plasma proteins. The combination of the basic *N*-methyl piperazine and aromatic rings led to an overlap with the well-known hERG pharmacophore and thus to a substantial inhibition in a dofetilide binding assay.[24] Decreasing the activity on the hERG channel was possible by lowering lipophilicity (e.g., compounds **4d** and **6d**) assessed by a high-throughput (HT-) logP assay,[25] but a complete suppression, a clear project requirement, could not be achieved for these basic piperazine

DOI: 10.1021/acsmedchemlett.6b00119
ACS Med. Chem. Lett. 2016, 7, 762−767

Table 5. PK parameters[a] for compound 11

species	rat[b]	rat[b]	rat[b]	dog[c]	dog[c]
dose [mg·kg^{-1}]	1 (iv)	3 (po)	30 (po)	0.1 (iv)	0.3 (po)
CL [mL·min^{-1}·kg^{-1}]	15 (3)			13 (3)	
V_{SS} [L·kg^{-1}]	2.0 (0.3)			1.0 (0.2)	
$t_{1/2}$ term. [h]	2.0 (0.5)			0.9 (0.1)	
AUC d.n.[d] [nM·h]	2315 (537)	500 (168)	237 (24)	2798 (715)	1188 (251)
BAV [%]		22 (7)	10 (1)		42 (9)
C_{max} d.n.[d] [nM]		48 (14)	20 (4)		440 (112)
T_{max} [h]		3.5 (3.1)	5.3 (2.2)		0.8 (0.3)

[a]Mean values (rat, n = 4; dog, n = 3) with standard deviation in brackets. [b]Female. [c]Male. [d]d.n. = dose normalized to 1 mg·kg^{-1}.

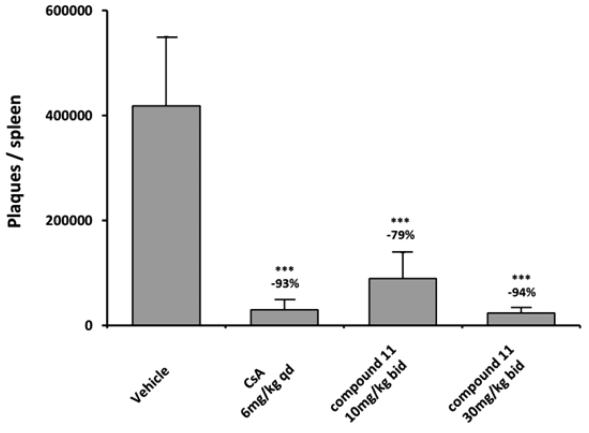

Figure 3. Dose-dependent inhibition of SRBC-specific IgM response by compound **11**; error bars indicate standard deviation; ***p < 0.001 compared to vehicle (student's t test, two-tailed distribution).

amides. Modulation of the microsomal turnover[26] for these derivatives also turned out to be possible to some degree, although overall clearance still remained high. In a rat PK experiment, compound **6d** showed substantial clearance (CL = 33 mL·min^{-1}·kg^{-1}, see Supplementary Table 1). Metabolite identification studies with **6d** suggested major metabolism around the piperazine moiety leading us to conclude that a major clearance reduction would not be possible without modifying this metabolic weak spot, ultimately leading to the introduction of a second amide functionality (Table 3). Pyridine **6e** and piperidine **6f** illustrate that the bridging phenyl ring can also be replaced by saturated or unsaturated heterocyclic rings, but as for all other analogues the impact on hERG and metabolism remained moderate.

We then discovered that the terminal piperazine *N*-methyl group could be substituted by short acyl groups. Table 3 outlines that *N*-acetyl piperazines **7**, **8**, **9**, and **11** show an excellent potency profile on PI3Kδ and selectivity profile over other PI3K isoforms. As for the *N*-methyl piperazine **5d**, addition of a *meta*-CF_3 group in the position-6 aromatic ring of the quinazoline was detrimental to isoform selectivity (compound **10**), presumably due to an H-bond between one of the fluorine atoms and the catalytic lysine. Due to the increased PSA of bis-amides compared to their monoamide counterparts we noticed that PAMPA effective permeability ($logP_e$ in 10^{-6} cm·s^{-1})[27] at neutral pH dropped and that translation into cellular assays needed to be closely monitored. Compound **7** shows a >5-fold potency drop in the mouse splenocyte assay, a trend we noticed also for other compounds with HT-logP around 3 or above (data not shown), presumably due to an increased likelihood for unspecific binding. These observations led us to preferentially place compounds into the HT-logP window between 2 and 3 to increase our chances for success. Bis-amides **7**−**11** are neutral and do not show any activity on the hERG channel up to 30 μM. For many compounds, the piperazine acylation also led to significant metabolic stability increase in microsomal preparations.

As already mentioned, our initial design hypothesis to achieve isoform selectivity was based on forming a salt bridge between the ligand and D832. Neutral derivatives like acetylated piperazines **7**−**11** are not able to offer a hydrogen bond donor, and we were initially surprised by the observed selectivity. In order to elucidate the molecular reason, we cocrystallized compound **11** with PI3Kα and PI3Kδ, and these structures have been determined to 3 and 2.9 Å, respectively (see Supporting Information). In general, the structures reveal an overall fold similar to previous structures solved in complex with other inhibitors.[28] The ligand is bound in the ATP site of the kinase domains and forms an identical, direct hydrogen bond to V828 (δ) or V850 (α) in the hinge and with K779 (δ) or K802 (α) in the affinity-pocket of the active site (see Supplementary Figure 2). Water-mediated hydrogen bonds are formed with the side chain oxygens of D787 and Y813 in the affinity pocket and with the backbone carbonyl oxygen of S813 at the ATP binding site cleft, as observed in the slightly better resolved PI3Kδ structure. The acetyl-piperazine group of the ligand stacks to W760 in the PI3Kδ structure (Figure 1, right panel), which leads to strong attractive dispersion forces. In PI3Kα, this interaction is not possible because R770, in contrast to the smaller T750 in the δ isoform, blocks the access to the corresponding tryptophan W780, and the ligand protrudes from the ATP binding pocket in an extended conformation (Figure 1, left panel). The solvent-exposed, electrostatic interaction between R770 and compound **11** in PI3Kα cannot compensate the van der Waals interactions between the acetyl-piperazine ring and the protein in the PI3Kδ complex resulting in a preference of compound **11** for the PI3Kδ isoform. Force field refinements of the original coordinates[29,30] induced only minor local changes and provide further support for these observations. Binding free energies that were calculated by MM/GBSA computations on the energy-refined crystal structures of compound **11**, using the Amber Generalized-Born (GB) options igb = 2 or 5 confirm a preference of PI3Kδ by 1.7 (igb = 5) to 2.1 (igb = 2) kcal/mol.[31]

Compound **11** showed selectivity against three lipid kinases, 40 protein kinases, and 36 targets of an internal safety panel (full list, see Supporting Information). As it was the compound with the most promising overall in vitro profile, it was selected for further pharmacological characterization including its effects on isoform-dependent immune cell function. Since PI3Kδ has been described as essential for B cell activation and function,[14,32,33] we measured the effect of compound **11** on human and rodent B cell activation. Our data demonstrate a consistent and potent inhibition of PI3Kδ-mediated B cell functions across different species (Table

DOI: 10.1021/acsmedchemlett.6b00119
ACS Med. Chem. Lett. 2016, 7, 762−767

4). Proximal readout parameters such as pAkt were equally well inhibited as further downstream events such as surface activation markers CD69/CD86 or proliferation.

To assess whether compound **11** was suitable for in vivo studies, we tested its pharmacokinetic properties in rats and dogs (Table 5). At an oral dose of 3 mg/kg, compound **11** showed a moderate 22% oral bioavailability in rats. While a higher total exposure could be reached with increasing the dose to 30 mg/kg, this overall gain was not dose-linear, and bioavailability dropped to 10%, likely due to solubility limited absorption. In dogs, overall pharmacokinetic properties for compound **11** were similar (low clearance and low volume of distribution), with a somewhat better 42% oral bioavailability at 0.3 mg/kg. Overall, we concluded that compound **11** had adequate pharmacokinetic properties to assess the translation of inhibiting B cell activation in vitro to the in vivo situation. To this end, PK/PD studies were performed in rodents following a single oral dose of compound **11** (30 mg/kg) in male Lewis rats. Blood was collected at various time points, and changes for two PD biomarker expression profiles as well as drug levels were determined (Figure 2). In agreement with the PK experiment in Sprague–Dawley (SD) rats, compound concentration in Lewis rat blood reached a maximum after 2 h with blood levels around 5 μM. A clear relationship of drug exposure and inhibition of Akt phosphorylation and anti-IgM/rIL-4-induced CD86 expression was observed. Within the test samples, the highest pAkt inhibition (88%) was observed 6 h after compound administration, whereas inhibition of CD86 expression was at its maximum of 71% already after 2 h.

As a consequence of these encouraging results on the proximal PD markers, compound **11** was profiled in an ex vivo plaque forming cell (PFC) assay.[34] This mechanistic assay quantitatively determines the antibody-producing B cell response following immunization with sheep red blood cells (SRBC). After 4 days of compound treatment, rats were sacrificed, and inhibition of plaques formed due to the SRBC specific B cell antibody response was assessed via the PFC assay (Figure 3). At a dose of 10 mg/kg bid, plaque formation (vehicle mean 4.18×10^5 PFC/spleen) was inhibited by 79% (95% confidence interval [CI] = 56 to 92 percentage points, $p < 0.001$). At 30 mg/kg bid, an inhibition of 94% (95% CI = 89 to 97 percentage points, $p < 0.001$) was achieved comparable to the inhibition seen with the positive control CsA (Cyclosporin A, 95% CI = 84 to 98 percentage points, $p < 0.001$). Full statistics can be found in the Supporting Information.

In summary, we have identified novel quinazoline based PI3Kδ selective inhibitors that we could optimize into cellularly potent derivatives. With compound **11** we profiled a candidate with good basic pharmacokinetic properties; however, we observed an underproportional exposure increase at higher doses very likely caused by limited solubility. Compound **11** demonstrated that the PI3Kδ-dependent inhibition of B cell activation observed in vitro and in rodent PK/PD studies translates into the full inhibition of B cell function, namely, the T-dependent specific antibody response in vivo. These results confirmed our initial target hypothesis and encouraged us to continue our search for a suitable development candidate.

■ ASSOCIATED CONTENT

Supporting Information

The Supporting Information is available free of charge on the ACS Publications website at DOI: 10.1021/acsmedchemlett.6b00119.

Full descriptions of all biological assays and in vivo studies. Characterization of all compounds. Full experimental procedures for the sequence leading to compound **11**. Crystallographic data collection and refinement statistics for crystal structures (PDF)

Accession Codes

PDB codes for X-ray crystal structures described in this study have been deposited in the Protein Data Bank under the following accession codes: 5IS5 (compound **11** in complex with PI3Kδ) and 5ITD (compound **11** in complex with PI3Kα).

■ AUTHOR INFORMATION

Corresponding Authors

*(K.H.) Tel: +41 79 6181814. E-mail: klemens.hoegenauer@novartis.com.

*(N.S.) Tel: +41 79 8451506. E-mail: nicolas.soldermann@novartis.com.

Notes

The authors declare no competing financial interest.

■ ACKNOWLEDGMENTS

We thank I. Adam, J. Andre, I. Jeulin, D. Rageot, R. Strang, B. Thai, and V. Tucconi for their synthetic contributions, D. Fabbro, D. Haasen, A. Hinz, U. McKeever, and P. Schmutz for their efforts towards developing and running biochemical and cellular assays, C. Beerli for pharmacokinetic assay work, B. Shrestha for protein expression, R. Elling for crystallography support, and N. G. Cooke and G. Weckbecker for scientific guidance. We are grateful to the MX beamline team at the Swiss Light Source (PSI Villigen, Switzerland) for outstanding support at the beamline and Expose GmbH (Switzerland) for diffraction data collection.

■ ABBREVIATIONS

BAV, absolute oral bioavailability; hERG, human ether-à-go-go-related gene; MM/GBSA, molecular mechanics energies combined with the generalized Born and surface area continuum solvation method; mTOR, mechanistic target of rapamycin; PFC, plaque forming cell(s); PI3K, phosphoinositide-3-kinase; SD rats, Sprague–Dawley rats; SRBC, sheep red blood cell(s)

■ REFERENCES

(1) Cantley, L. C. The Phosphoinositide 3-Kinase Pathway. *Science* **2002**, *296* (5573), 1655–1657.

(2) Hawkins, P. T.; Stephens, L. R. PI3K Signalling in Inflammation. *Biochim. Biophys. Acta, Mol. Cell Biol. Lipids* **2015**, *1851* (6), 882–897.

(3) Geering, B.; Cutillas, P. R.; Nock, G.; Gharbi, S. I.; Vanhaesebroeck, B. Class IA Phosphoinositide 3-Kinases Are Obligate p85-p110 Heterodimers. *Proc. Natl. Acad. Sci. U. S. A.* **2007**, *104* (19), 7809–7814.

(4) Marone, R.; Cmiljanovic, V.; Giese, B.; Wymann, M. P. Targeting Phosphoinositide 3-kinase—Moving towards Therapy. *Biochim. Biophys. Acta, Proteins Proteomics* **2008**, *1784* (1), 159–185.

(5) Maira, S.-M.; Voliva, C.; Garcia-Echeverria, C. Class IA Phosphatidylinositol 3-Kinase: From Their Biologic Implication in Human Cancers to Drug Discovery. *Expert Opin. Ther. Targets* **2008**, *12* (2), 223–238.

(6) Foster, J. G.; Blunt, M. D.; Carter, E.; Ward, S. G. Inhibition of PI3K Signaling Spurs New Therapeutic Opportunities in Inflammatory/Autoimmune Diseases and Hematological Malignancies. *Pharmacol. Rev.* **2012**, *64* (4), 1027–1054.

(7) Rommel, C.; Camps, M.; Ji, H. PI3Kδ and PI3Kγ: Partners in Crime in Inflammation in Rheumatoid Arthritis and Beyond? *Nat. Rev. Immunol.* **2007**, *7* (3), 191–201.

DOI: 10.1021/acsmedchemlett.6b00119
ACS Med. Chem. Lett. 2016, 7, 762–767

(8) Stark, A.-K.; Sriskantharajah, S.; Hessel, E. M.; Okkenhaug, K. PI3K Inhibitors in Inflammation, Autoimmunity and Cancer. *Curr. Opin. Pharmacol.* **2015**, *23*, 82−91.
(9) Hirsch, E.; Katanaev, V. L.; Garlanda, C.; Azzolino, O.; Pirola, L.; Silengo, L.; Sozzani, S.; Mantovani, A.; Altruda, F.; Wymann, M. P. Central Role for G Protein-Coupled Phosphoinositide 3-Kinase γ in Inflammation. *Science* **2000**, *287* (5455), 1049−1053.
(10) Li, Z.; Jiang, H.; Xie, W.; Zhang, Z.; Smrcka, A. V.; Wu, D. Roles of PLC-β2 and -β3 and PI3Kγ in Chemoattractant-Mediated Signal Transduction. *Science* **2000**, *287* (5455), 1046−1049.
(11) Patrucco, E.; Notte, A.; Barberis, L.; Selvetella, G.; Maffei, A.; Brancaccio, M.; Marengo, S.; Russo, G.; Azzolino, O.; Rybalkin, S. D.; Silengo, L.; Altruda, F.; Wetzker, R.; Wymann, M. P.; Lembo, G.; Hirsch, E. PI3Kγ Modulates the Cardiac Response to Chronic Pressure Overload by Distinct Kinase-Dependent and -Independent Effects. *Cell* **2004**, *118* (3), 375−387.
(12) Clayton, E.; Bardi, G.; Bell, S. E.; Chantry, D.; Downes, C. P.; Gray, A.; Humphries, L. A.; Rawlings, D.; Reynolds, H.; Vigorito, E.; Turner, M. A Crucial Role for the PI3Kδ Subunit of Phosphatidylinositol 3-Kinase in B Cell Development and Activation. *J. Exp. Med.* **2002**, *196* (6), 753−763.
(13) Jou, S.-T.; Carpino, N.; Takahashi, Y.; Piekorz, R.; Chao, J.-R.; Carpino, N.; Wang, D.; Ihle, J. N. Essential, Nonredundant Role for the Phosphoinositide 3-Kinase p110δ in Signaling by the B-Cell Receptor Complex. *Mol. Cell. Biol.* **2002**, *22* (24), 8580−8591.
(14) Okkenhaug, K.; Bilancio, A.; Farjot, G.; Priddle, H.; Sancho, S.; Peskett, E.; Pearce, W.; Meek, S. E.; Salpekar, A.; Waterfield, M. D.; Smith, A. J. H.; Vanhaesebroeck, B. Impaired B and T Cell Antigen Receptor Signaling in p110δ PI 3-Kinase Mutant Mice. *Science* **2002**, *297* (5583), 1031−1034.
(15) Sadhu, C.; Masinovsky, B.; Dick, K.; Sowell, C. G.; Staunton, D. E. Essential Role of Phosphoinositide 3-Kinase δ in Neutrophil Directional Movement. *J. Immunol.* **2003**, *170* (5), 2647−2654.
(16) Park, S. J.; Lee, K. S.; Kim, S. R.; Min, K. H.; Moon, H.; Lee, M. H.; Chung, C. R.; Han, H. J.; Puri, K. D.; Lee, Y. C. Phosphoinositide 3-Kinase δ Inhibitor Suppresses Interleukin-17 Expression in a Murine Asthma Model. *Eur. Respir. J.* **2010**, *36* (6), 1448−1459.
(17) Durand, C. A.; Richer, M. J.; Brenker, K.; Graves, M.; Shanina, I.; Choi, K.; Horwitz, M. S.; Puri, K. D.; Gold, M. R. Selective Pharmacological Inhibition of Phosphoinositide 3-Kinase p110delta Opposes the Progression of Autoimmune Diabetes in Non-Obese Diabetic (NOD) Mice. *Autoimmunity* **2013**, *46* (1), 62−73.
(18) Norman, P. Selective PI3Kδ Inhibitors, a Review of the Patent Literature. *Expert Opin. Ther. Pat.* **2011**, *21* (11), 1773−1790.
(19) Bui, M.; Hao, X.; Shin, Y.; Cardozo, M.; He, X.; Henne, K.; Suchomel, J.; McCarter, J.; McGee, L. R.; San Miguel, T.; Medina, J. C.; Mohn, D.; Tran, T.; Wannberg, S.; Wong, J.; Wong, S.; Zalameda, L.; Metz, D.; Cushing, T. D. Synthesis and SAR Study of Potent and Selective PI3Kδ Inhibitors. *Bioorg. Med. Chem. Lett.* **2015**, *25* (5), 1104−1109.
(20) Cushing, T. D.; Hao, X.; Shin, Y.; Andrews, K.; Brown, M.; Cardozo, M.; Chen, Y.; Duquette, J.; Fisher, B.; Gonzalez-Lopez de Turiso, F.; He, X.; Henne, K. R.; Hu, Y.-L.; Hungate, R.; Johnson, M. G.; Kelly, R. C.; Lucas, B.; McCarter, J. D.; McGee, L. R.; Medina, J. C.; San Miguel, T.; Mohn, D.; Pattaropong, V.; Pettus, L. H.; Reichelt, A.; Rzasa, R. M.; Seganish, J.; Tasker, A. S.; Wahl, R. C.; Wannberg, S.; Whittington, D. A.; Whoriskey, J.; Yu, G.; Zalameda, L.; Zhang, D.; Metz, D. P. Discovery and in Vivo Evaluation of (S)-N-(1-(7-Fluoro-2-(pyridin-2-Yl)quinolin-3-Yl)ethyl)-9H-Purin-6-Amine (AMG319) and Related PI3Kδ Inhibitors for Inflammation and Autoimmune Disease. *J. Med. Chem.* **2015**, *58* (1), 480−511.
(21) Shin, Y.; Suchomel, J.; Cardozo, M.; Duquette, J.; He, X.; Henne, K.; Hu, Y.-L.; Kelly, R. C.; McCarter, J.; McGee, L. R.; Medina, J. C.; Metz, D.; San Miguel, T.; Mohn, D.; Tran, T.; Vissinga, C.; Wong, S.; Wannberg, S.; Whittington, D. A.; Whoriskey, J.; Yu, G.; Zalameda, L.; Zhang, X.; Cushing, T. D. Discovery, Optimization, and in Vivo Evaluation of Benzimidazole Derivatives AM-8508 and AM-9635 as Potent and Selective PI3Kδ Inhibitors. *J. Med. Chem.* **2016**, *59* (1), 431−447.
(22) Maira, S.-M.; Stauffer, F.; Brueggen, J.; Furet, P.; Schnell, C.; Fritsch, C.; Brachmann, S.; Chène, P.; Pover, A. D.; Schoemaker, K.; Fabbro, D.; Gabriel, D.; Simonen, M.; Murphy, L.; Finan, P.; Sellers, W.; García-Echeverría, C. Identification and Characterization of NVP-BEZ235, a New Orally Available Dual Phosphatidylinositol 3-Kinase/mammalian Target of Rapamycin Inhibitor with Potent in Vivo Antitumor Activity. *Mol. Cancer Ther.* **2008**, *7* (7), 1851−1863.
(23) Camps, M.; Ruckle, T.; Ji, H.; Ardissone, V.; Rintelen, F.; Shaw, J.; Ferrandi, C.; Chabert, C.; Gillieron, C.; Francon, B.; Martin, T.; Gretener, D.; Perrin, D.; Leroy, D.; Vitte, P.-A.; Hirsch, E.; Wymann, M. P.; Cirillo, R.; Schwarz, M. K.; Rommel, C. Blockade of PI3Kγ Suppresses Joint Inflammation and Damage in Mouse Models of Rheumatoid Arthritis. *Nat. Med.* **2005**, *11* (9), 936−943.
(24) Finlayson, K.; Turnbull, L.; January, C. T.; Sharkey, J.; Kelly, J. S. [3H]Dofetilide Binding to HERG Transfected Membranes: A Potential High Throughput Preclinical Screen. *Eur. J. Pharmacol.* **2001**, *430* (1), 147−148.
(25) Faller, B.; Grimm, H. P.; Loeuillet-Ritzler, F.; Arnold, S.; Briand, X. High-Throughput Lipophilicity Measurement with Immobilized Artificial Membranes. *J. Med. Chem.* **2005**, *48* (7), 2571−2576.
(26) Trunzer, M.; Faller, B.; Zimmerlin, A. Metabolic Soft Spot Identification and Compound Optimization in Early Discovery Phases Using MetaSite and LC-MS/MS Validation. *J. Med. Chem.* **2009**, *52* (2), 329−335.
(27) Faller, B. Artificial Membrane Assays to Assess Permeability. *Curr. Drug Metab.* **2008**, *9* (9), 886−892.
(28) Berndt, A.; Miller, S.; Williams, O.; Le, D. D.; Houseman, B. T.; Pacold, J. I.; Gorrec, F.; Hon, W.-C.; Liu, Y.; Rommel, C.; Gaillard, P.; Ruckle, T.; Schwarz, M. K.; Shokat, K. M.; Shaw, J. P.; Williams, R. L. The p110δ Crystal Structure Uncovers Mechanisms for Selectivity and Potency of Novel PI3K Inhibitors. *Nat. Chem. Biol.* **2010**, *6* (2), 117−124.
(29) Maier, J. A.; Martinez, C.; Kasavajhala, K.; Wickstrom, L.; Hauser, K. E.; Simmerling, C. ff14SB: Improving the Accuracy of Protein Side Chain and Backbone Parameters from ff99SB. *J. Chem. Theory Comput.* **2015**, *11* (8), 3696−3713.
(30) Wang, J.; Wolf, R. M.; Caldwell, J. W.; Kollman, P. A.; Case, D. A. Development and Testing of a General Amber Force Field. *J. Comput. Chem.* **2004**, *25* (9), 1157−1174.
(31) Case, D. A.; Berryman, J. T.; Betz, R. M.; Cerutti, D. S.; Cheatham, T. E., III; Darden, T. A.; Duke, R. E.; Giese, T. J.; Gohlke, H.; Goetz, A. W.; Homeyer, N.; Izadi, S.; Janowski, P.; Kaus, J.; Kovalenko, A.; Lee, T. S.; LeGrand, S.; Li, P.; Luchko, T.; Luo, R.; Madej, B.; Merz, K. M.; Monard, G.; Needham, P.; Nguyen, H.; Nguyen, H. T.; Omelyan, I.; Onufriev, A.; Roe, D. R.; Roitberg, A.; Salomon-Ferrer, R.; Simmerling, C. L.; Smith, W.; Swails, J.; Walker, R. C.; Wang, J.; Wolf, R. M.; Wu, X.; York, D. M.; Kollman, P. A. *AMBER 2015*; University of California: San Francisco, 2015.
(32) Pinho, V.; de Castro Russo, R.; Amaral, F. A.; de Sousa, L. P.; Barsante, M. M.; de Souza, D. G.; Alves-Filho, J. C.; Cara, D. C.; Hayflick, J. S.; Rommel, C.; Ruckle, T.; Rossi, A. G.; Teixeira, M. M. Tissue- and Stimulus-Dependent Role of Phosphatidylinositol 3-Kinase Isoforms for Neutrophil Recruitment Induced by Chemoattractants In Vivo. *J. Immunol.* **2007**, *179* (11), 7891−7898.
(33) Soond, D. R.; Bjørgo, E.; Moltu, K.; Dale, V. Q.; Patton, D. T.; Torgersen, K. M.; Galleway, F.; Twomey, B.; Clark, J.; Gaston, J. S. H.; Taskén, K.; Bunyard, P.; Okkenhaug, K. PI3K p110δ Regulates T-Cell Cytokine Production during Primary and Secondary Immune Responses in Mice and Humans. *Blood* **2010**, *115* (11), 2203−2213.
(34) Jerne, N. K.; Nordin, A. A. Plaque Formation in Agar by Single Antibody-Producing Cells. *Science* **1963**, *140* (3565), 405−405.

DOI: 10.1021/acsmedchemlett.6b00119
ACS Med. Chem. Lett. 2016, 7, 762−767